

Operculina and *Neoassilina*: A Revision of Recent Nummulitid Genera Based on Molecular and Morphological Data Reveals a New Genus

Maria Holzmann^{1*}, Johann Hohenegger², Laure Apothéloz-Perret-Gentil^{1, 6}, Raphael Morard³, Sigal Abramovich⁴, Danna Titelboim⁴, Jan Pawlowski^{1, 5, 6}

1. Department of Genetics and Evolution, University of Geneva, 1211 Geneva 4, Switzerland


2. Department of Paleontology, Geozentrum, 1090 Wien, Austria

3. MARUM Center for Marine Environmental Sciences, University of Bremen, 28359 Bremen, Germany

4. Department of Geological and Environmental Sciences, Ben Gurion University of the Negev, Beer Sheva 84105, Israel

5. Institute of Oceanology, Polish Academy of Sciences, Sopot, Poland

6. ID-GenE Ecodiagnostics, 1202 Geneva, Switzerland

 Maria Holzmann: <https://orcid.org/0000-0003-2460-6210>

ABSTRACT: The genus *Operculina*, a large symbiont-bearing benthic foraminifer, is characterized by high morphological variability showing thick involute to intermediate semi-involute to flat evolute tests. Different morphotypes are either considered as ecophenotypes or distinct species. In order to test the hypothesis of ecophenotypes versus different species, a single cell high throughput sequencing approach was applied to assess the interspecific diversity of *Operculina*. This results in two groups of ribotypes, one corresponding to *Operculina ammonoides*/*Operculina discoidalis*, the other containing *Operculina complanata*/*Operculina elegans*. These groups can also be separated morphologically. Therefore, *O. complanata* and *O. elegans* represent a single species and the latter can be regarded as a junior synonym of *O. complanata*. *Operculina ammonoides* and *O. discoidalis* also form a single species, which makes the latter a junior synonym of *O. ammonoides*. Because generic differences in *Operculina* species are manifested in morphology and molecular genetics, the genus *Neoassilina* with the designated species *Neoassilina ammonoides* is installed. Additional analysis of ribosomal SSU rDNA data of eight recent nummulitid genera confirms the obtained high throughput sequencing results and further shows that *Palaeonummulites venosus* builds a clade with *O. complanata* that branches at the base of other Nummulitidae containing *Planostegina*, *Planoperculina*, *Cycloclypeus*, *Heterostegina*, *Operculinella* and *Neoassilina*.

KEY WORDS: *Operculina*, *Neoassilina*, Nummulitidae, interspecific diversity, SSU rDNA, morphology.

0 INTRODUCTION

Nummulitidae are a group of large benthic foraminifera (LBF) that inhabit tropical and subtropical regions of the Indopacific. They are characterized by planispiral, evolute to involute tests, annular chambers that may be divided into chamberlets, subsutural canals, a spiral marginal cord and a spiral or intraseptal canal system (Loeblich and Tappan, 1988). Only the genus *Heterostegina* is also present in the Caribbean (Hohenegger and Yordanova, 2000; Langer and Hottinger, 2000). The classification of Nummulitidae is based on morphologic characters such as growth form, ornamentation and internal test

characters (Yordanova and Hohenegger, 2004; Hottinger, 1977). The family was traditionally divided into the subfamilies Nummulitinae and Heterostegininae based on the presence or absence of chamberlets (Banner and Hodgkinson, 1991). Molecular data not only have confirmed the monophyly of the family but also shown that chamber subdivision has arisen independently in several lineages (Holzmann and Pawlowski, 2017; Holzmann et al., 2003).

Like all members of LBF, Nummulitidae harbor endosymbiotic algae and are therefore restricted to the euphotic zone. Nummulitidae establish symbiotic relationships with diatoms (Lee et al., 1989). Their molecular identification has revealed a close relationship to the genus *Thalassionema* (Holzmann et al., 2006). Diatom symbionts of deep water and shallow water nummulitids cluster in different clades supporting a depth zonation (Holzmann et al., 2006).

Nummulitid distribution in reef environments is dependent on light intensity, substrate and wave activity and they

*Corresponding author: maria.holzmann@unige.ch

© The Authors 2022. This article is published with open access at Springerlink.com

Manuscript received August 6, 2021.

Manuscript accepted December 2, 2021.

show a range of morphological adaptations to different environments such as thickening/flattening of tests or increase/decrease of external ornamentations (Hohenegger, 2006, 2004; Beavington-Penney and Racey, 2004). Morphological variability is especially high in the genus *Operculina* and has been interpreted either as an adaptation to changing environmental conditions (ecophenotypes) or different morphotypes have been recognized as distinct species (Oron et al., 2018; Hohenegger, 2011, 2000; Yordanova and Hohenegger, 2004; Pecheux, 1995; Reiss and Hottinger, 1984). *Operculina ammonoides* is characterized by planispiral tests that are either thick/involute or thin/evolute. Intermediate semi-involute morphotypes are also abundant (Oron et al., 2018). Reiss and Hottinger (1984) noted that *O. ammonoides* occurs between 20 and 130 m depth in the Gulf of Aqaba. Involute specimens were frequent between 50 and 80 m whereas evolute specimens were abundant between 70 and 100 m depth. Specimens living below 60 m depth were distinguished by interseptal pillars forming bumps on the shell surface. These surface ornaments were viewed as lenses focusing the dwindling light and enabling thus the symbionts to continue their photosynthetic activity (Hottinger, 2006a, b).

Hohenegger (2006) stated that *O. ammonoides* is restricted to shallower environments in the West Pacific and competes with *O. complanata* in the deeper parts. The latter species is absent from the Red Sea and Indian Ocean where *O. ammonoides* also colonizes the deeper photic zones. Beavington-Penney and Racey (2004) note that *O. ammonoides* and *O. complanata* occur down to the deepest photic zone, which corresponds to less than 1% of surface light intensity, while *O. discoidalis* prefers medium light conditions corresponding to 10% surface light intensity.

Most authors consider different morphotypes of *O. ammonoides* as ecophenotypes (Oron et al., 2018; Pecheux, 1995; Reiss and Hottinger, 1984). Reiss and Hottinger (1984) stated that measurements of internal characters did not yield significant differences in various morphotypes and Oron et al. (2018) observed phenotypic changes in specimens that were subjected to different light conditions. Involute specimens would construct evolute thinner chambers when relocated to deeper settings. Yordanova and Hohenegger (2004) noted that flattening of the tests can be observed in *O. ammonoides*, *O. elegans* and *O. complanata* with increasing depth. The different morphotypes of *O. ammonoides* are regarded as separate species according to the thickness/diameter relations showing a clear gap between involute and evolute specimens. *Operculina elegans* and *O. complanata* from shallow water areas display the same ornamentation consisting of surface knobs covering the inner chambers and turning to large bosses in the umbilical area. *Operculi-*

na complanata specimens from deeper water show a different surface ornamentation with septa being covered by tiny knobs and chamber walls being studded with pustules (Yordanova and Hohenegger, 2004). Hohenegger (2011) argued that the only morphological difference between *O. elegans* and *O. complanata* is septal undulation which could be a response to different environmental conditions and suggests that they represent ecophenotypes belonging to a single species. Hohenegger (2011) further assumed that *O. discoidalis* and *O. ammonoides* are ecophenotypes of one species based on their close morphological relation.

We tested the hypothesis of ecophenotypes versus species by investigating the interspecific variability of four *Operculina* species (*O. ammonoides*, *O. elegans*, *O. complanata*, *O. discoidalis*) using a single cell high throughput sequencing (HTS) approach (Pawlowski et al., 2014) coupled with morphological examination. Additional ribosomal sequences (complete SSU rDNA and SSU rDNA barcoding fragment) were acquired for these species as well as for six other nummulitid genera (*Palaeonummulites*, *Operculinella*, *Heterostegina*, *Planostegina*, *Planoperculina*, *Cyclochypus*). The obtained molecular results confirm the presence of two groups that are not closely related, one consisting of *O. ammonoides/O. discoidalis*, the other containing *O. complanata/O. elegans*. Within each group, species pairs are genetically identical and have overlapping morphological characteristics. We can therefore affirm the presence of ecophenotypes in both groups and propose a revision of the genus *Operculina* and the installation of the genus *Neoassilina* based on molecular and morphological results.

1 MATERIAL AND METHODS

1.1 Sampling

Living nummulitid specimens used in the present study were collected from the West Pacific (Japan, Philippines) and the Red Sea (Israel) (Table 1). Sampling was carried out at 20, 23 and 45 m by dredging, SCUBA diving or snorkeling. Living specimens were identified by brownish protoplasmic coloration due to endosymbiotic diatoms, isolated under a binocular and cleaned with a brush (Holzmann et al., 2003). Specimens identified as *Operculina* spp. were photographed with a Leica M205C motorized stereomicroscope equipped with a Leica DFC450C camera.

1.2 Morphology

Identification of species for molecular genetic analysis has been done with qualitative (nominal scaled) and meristic (rational scaled) data. Surface structures of the test consist of umbonal plugs and small to large papillae, the former can lead to beams (see Hottinger, 2006a, b).

Table 1 List of nummulitids for which complete or partial (barcoding) SSU rDNA sequences were obtained

Species	Isolate	Sampling locality	Accession numbers SSU rDNA	Morphological identification
<i>Neoassilina ammonoides</i> *	8	Sesoko, Japan	AJ879147	<i>Operculina discoidalis</i>
<i>Neoassilina ammonoides</i> +	232	Sesoko, Japan	AJ488888, DQ440525	<i>Operculina ammonoides</i>
<i>Neoassilina ammonoides</i> +	253	Sesoko, Japan	AJ879130 , AJ488889	<i>Operculina discoidalis</i>
<i>Neoassilina ammonoides</i> +	494	Lizard Island, Australia	AJ488887, DQ440526	<i>Operculina ammonoides</i>

Table 1 Continued

Species	Isolate	Sampling locality	Accession numbers SSU rDNA	Morphological identification
<i>Neoassilina ammonoides</i> *+	19231	Eilat, Israel	MW816127, MW816128	<i>Operculina ammonoides</i>
<i>Neoassilina ammonoides</i> *+	19232	Eilat, Israel	MW816129, MW816130	<i>Operculina ammonoides</i>
<i>Neoassilina ammonoides</i> *+	19233	Eilat, Israel	MW816131, MW816132	<i>Operculina ammonoides</i>
<i>Neoassilina ammonoides</i> *+	19234	Eilat, Israel	MW816133, MW816134	<i>Operculina ammonoides</i>
<i>Neoassilina ammonoides</i> *	19235	Eilat, Israel	MW816135	<i>Operculina ammonoides</i>
<i>Neoassilina ammonoides</i> *+	19236	Eilat, Israel	MW816136	<i>Operculina ammonoides</i>
<i>Neoassilina ammonoides</i> *+	19237	Eilat, Israel	MW816137	<i>Operculina ammonoides</i>
<i>Neoassilina ammonoides</i> *	19993	Eilat, Israel	MT913380	<i>Operculina ammonoides</i>
<i>Cycloclypeus carpenteri</i> +	21	Sesoko, Japan	AJ879133	
<i>Cycloclypeus carpenteri</i> +	659	Minna Jima, Japan	AJ488885	
<i>Heterostegina depressa</i> *	3	Sesoko, Japan	AJ879131	
<i>Heterostegina depressa</i> *	27	Amami-O-Shima, Japan	AJ879138	
<i>Heterostegina depressa</i> *	39	Key Largo, Florida, USA	AJ879139	
<i>Heterostegina depressa</i> +	282	Florida Keys, USA	AJ488892	
<i>Heterostegina depressa</i> +	308	Western Australia	AJ879132 , AJ488891	
<i>Heterostegina depressa</i> *	377	Eilat, Israel	AJ488893	
<i>Heterostegina depressa</i> +	642	Helengeli, Maldives	AJ488890	
<i>Heterostegina depressa</i> *+	14668	Cabilao, Phillipines	MW816138, MW816139, MW816140	
<i>Heterostegina depressa</i> *+	14669	Cabilao, Phillipines	MW816141, MW816142	
<i>Heterostegina depressa</i> *+	14670	Cabilao, Phillipines	MW816143, MW816144	
<i>Heterostegina depressa</i> *+	14671	Cabilao, Phillipines	MW816145, MW816146	
<i>Operculina complanata</i> *	20	Sesoko, Japan	AJ879144	<i>Operculina complanata</i>
<i>Operculina complanata</i> *	48	Sesoko, Japan	AJ879143	<i>Operculina complanata</i>
<i>Operculina complanata</i> *	49	Sesoko, Japan	AJ879142	<i>Operculina complanata</i>
<i>Operculina complanata</i> *+	50	Sesoko, Japan	AY804333	<i>Operculina complanata</i>
<i>Operculina complanata</i> *	53	Sesoko, Japan	AJ879141	<i>Operculina elegans</i>
<i>Operculina complanata</i> *+	54	Sesoko, Japan	AJ879164	<i>Operculina elegans</i>
<i>Operculina complanata</i> *	19508	Sesoko, Japan	MT913352	<i>Operculina elegans</i>
<i>Operculina complanata</i> *	19528	Sesoko, Japan	MT913355	<i>Operculina elegans</i>
<i>Operculina complanata</i> *	19533	Sesoko, Japan	MT913353	<i>Operculina elegans</i>
<i>Operculina complanata</i> *	19549	Sesoko, Japan	MT913356	<i>Operculina elegans</i>
<i>Operculina complanata</i> *	19553	Sesoko, Japan	MT913354	<i>Operculina elegans</i>
<i>Operculinella cumingi</i> +	12	Sesoko, Japan	AJ879136	
<i>Operculinella cumingii</i> *	13	Sesoko, Japan	AJ879148	
<i>Palaeonummulites venosus</i> *	c9	Sesoko, Japan	MW813988	
<i>Palaeonummulites venosus</i> *	c10	Sesoko, Japan	MW813989	
<i>Palaeonummulites venosus</i> *	c11	Sesoko, Japan	MW813990	
<i>Palaeonummulites venosus</i> *	9	Sesoko, Japan	AJ879145	
<i>Palaeonummulites venosus</i> *	11	Sesoko, Japan	AJ879146	
<i>Palaeonummulites venosus</i> +	301	Sesoko, Japan	AJ318226	
<i>Planoperculina heterosteginoides</i> *+	17	Sesoko, Japan	AJ879135	
<i>Planostegina longisepta</i> *+	42	Amami-O-Shima, Japan	AJ879134	
<i>Planostegina operculinoides</i> +	16	Sesoko, Japan	AJ879140, DQ440527	
<i>Planostegina operculinoides</i> +	662	Minnu, Japan	AJ488886	
<i>Pararotalia nipponica</i> +	862	Shizuoka, Japan	AJ879137 , AJ488884	

*SSU rDNA sequences obtained for the present study; + PCR products cloned prior to sequencing; the remaining SSU rDNA sequences were published by Holzmann et al. (2003) and Holzmann and Pawlowski (2017); accession numbers in bold indicate complete SSU rDNA sequences.

Test shape of the last whorl was modeled by the logarithmic spiral

$$\text{radius} = \text{initial} \cdot \text{increase}^{\text{radians}} \quad (1)$$

Scale-independent marginal and umbilical radii of the last whorl were measured in distance of $\pi/2$, π , $3\pi/4$ and 2π (Fig. 1). The ratios ‘umbonal/marginal radii’ were fitted at the four revolution angles by the exponential function

$$\text{ratio}_{\text{umbonal/marginal}} = \text{ratio}_{\pi=0} \cdot \text{slope}^{\text{radians}} \quad (2)$$

Furthermore, percentages of umbonal to marginal radii were calculated at revolution angles $\pi/2$ and 2π . Differences between species were tested by discriminant analysis using PAST v. 4.06 (Hammer, 2021) and EXCEL.

1.3 DNA Extraction, PCR Amplification, Cloning and Sequencing

For the present study, DNA was extracted of 108 nummulitid specimens (Tables 1, 2) using the DNeasy Plant Mini Kit (Qiagen). The complete SSU rDNA was amplified in three overlapping fragments using semi-nested PCR. The 5' fragment was amplified with primers sA10 (ctcaagattaagccatgcaagtgg)-s12r (gktagtcttrmhagggtca) and sA10-s7r (ctgrttgttcacagtrttg). For the middle fragment primers s6f (cgcggtaataaccagtc)-s17r (cggtcacgttcgttg) and s6f-s15A (ctaagaacggccatgcaccacc) were used and for the 3'end fragment primers s14F3 (acgcamgtgtgaaacttg)-sB (tgatccttctcaggttcacctac) and s14F1 (aaggccaccacaagaacc)-sB were used. The 3'end fragment corresponds to the barcoding fragment in foraminifera (Pawlowski and Holzmann, 2014). Thirty-five and 25 cycles were performed for the initial and the semi-nested PCR respectively with an annealing temperature of 50 °C for the first PCR and 52 °C for the second PCR.

The amplified PCR products were purified using the High Pure PCR Cleanup Micro Kit (Roche Diagnostics). PCR products obtained from twenty-seven specimens were cloned prior

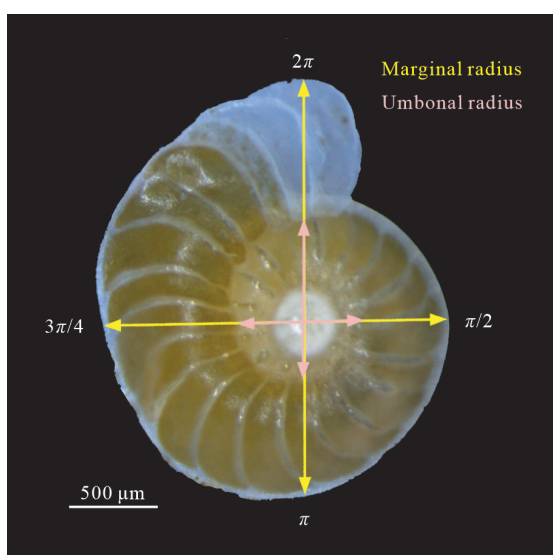


Figure 1. Radius measurements in the final whorl of *Operculina ammonoides* (now *Neoassilina ammonoides*, Ind. 258_1) from Israel, with few tiny papillae at the surface following the septal courses.

to sequencing (Table 1) using the TOPO TA Cloning Kit (Invitrogen) following the manufacturer’s instructions and transforming amplified PCR products into competent *Escherichia coli*. Sequencing reactions were performed using the BigDye Terminator v3.1 Cycle Sequencing Kit (Applied Biosystems). The newly acquired sequences were deposited in the EMBL/GenBank database (isolate and accession numbers are given in Table 1).

1.4 High Troughput Sequencing Analysis

In order to test the hypothesis of ecophenotypes versus distinct species in *Operculina*, we performed a HTS study on single specimens. The results allowed us to investigate intra-individual polymorphism for a range of selected specimens from different habitats and with different test shapes (Table 2). The 79 extractions of *Operculina* were amplified by semi-nested PCR using the primer pair s14F3 and s17r for the first and primers s14F1 and s17r for the second amplification. Thirty-five and 25 cycles were performed for the initial and the semi-nested PCR respectively with an annealing temperature of 50 °C for the first PCR and 52 °C for the second PCR. A unique combination of tags was used for each sample during the second PCR in order to multiplex them into Illumina libraries. Individual tags are composed of 8 nucleotides attached at each primer 5'-extremity (Esling et al., 2015). The PCR products were then quantified with capillary electrophoresis using a QIAxcel instrument (Qiagen). Equimolar concentrations of PCR products were pooled into three libraries and purified using High Pure PCR Product Purification Kit (Roche Applied Science). The library preparations were performed using Illumina TruSeq DNA PCR-Free Library Preparation Kit. Libraries were quantified with qPCR using KAPA Library Quantification Kit and sequenced on a MiSeq instrument using a MiSeq Reagent Nano Kit v2 with paired-end sequencing for 500 cycles and an expected outcome of 1 million sequences.

Raw FASTQ reads were demultiplexed to retrieve the R1 and R2 fastq files for each sample using the demultiplexer module implemented in SLIM (Dufresne et al., 2019). Quality filtering, removal of chimera and generation of the amplicon sequence variant (ASV) table were done using dada2 R package v.1.10.1 (Callahan et al., 2016). Contaminant ASVs (i.e., sequences belonging to other organisms than *Operculina*) and ASVs with a total number of reads below 100 were removed. The remaining ASVs were visualized in Seaview vs.4.3.3. alignment software (Gouy et al., 2010) and grouped into ribotypes. A ribotype was defined as a group of ASVs that diverge from a representative ASV (the most abundant ASV from each cluster) with at least 4 differences (substitution, insertion or deletion).

2 RESULTS

2.1 Morphological Analysis

Test shape and test surface structures were investigated in 60 individuals originally identified as *Operculina ammonoides* (Eilat, Israel, 20 and 45 m depth, Sesoko, Japan, 23 m depth) and 41 individuals originally identified as *Operculina elegans* (Sesoko, Japan, 23 m depth). Of the investigated specimens, 79 were used for molecular analysis (Table 2).

Table 2 List of nummulitids used for high throughput sequencing (HTS) analysis; all investigated specimens were photographed with a Leica M205C prior to extraction

Species	Isolate	Sampling locality	Test morphology	Morphological identification	Raw reads	Filtered reads
<i>Operculina complanata</i>	19507	Sesoko, Japan	Semi-involute	<i>Operculina elegans</i>	2501	2488
<i>Operculina complanata</i>	19508*	Sesoko, Japan	Semi-involute	<i>Operculina elegans</i>	5603	5588
<i>Operculina complanata</i>	19509	Sesoko, Japan	Evolute	<i>Operculina elegans</i>	2129	2122
<i>Operculina complanata</i>	19510	Sesoko, Japan	Evolute	<i>Operculina elegans</i>	6495	6469
<i>Operculina complanata</i>	19511	Sesoko, Japan	Evolute	<i>Operculina elegans</i>	6513	6463
<i>Operculina complanata</i>	19513	Sesoko, Japan	Evolute	<i>Operculina elegans</i>	6842	6806
<i>Operculina complanata</i>	19514	Sesoko, Japan	Evolute	<i>Operculina elegans</i>	2050	2031
<i>Operculina complanata</i>	19515	Sesoko, Japan	Evolute	<i>Operculina elegans</i>	4681	4650
<i>Operculina complanata</i>	19517	Sesoko, Japan	Semi-involute	<i>Operculina elegans</i>	2723	2716
<i>Operculina complanata</i>	19518	Sesoko, Japan	Evolute	<i>Operculina elegans</i>	9144	9101
<i>Operculina complanata</i>	19519	Sesoko, Japan	Evolute	<i>Operculina elegans</i>	40	32
<i>Operculina complanata</i>	19522	Sesoko, Japan	Evolute	<i>Operculina elegans</i>	3451	3436
<i>Operculina complanata</i>	19526	Sesoko, Japan	Evolute	<i>Operculina elegans</i>	7601	7581
<i>Operculina complanata</i>	19528*	Sesoko, Japan	Semi-involute	<i>Operculina elegans</i>	7405	6692
<i>Operculina complanata</i>	19529	Sesoko, Japan	Evolute	<i>Operculina elegans</i>	5014	4621
<i>Operculina complanata</i>	19530	Sesoko, Japan	Evolute	<i>Operculina elegans</i>	53022	52538
<i>Operculina complanata</i>	19531	Sesoko, Japan	Evolute	<i>Operculina elegans</i>	40017	39851
<i>Operculina complanata</i>	19532	Sesoko, Japan	Evolute	<i>Operculina elegans</i>	10522	10450
<i>Operculina complanata</i>	19533*	Sesoko, Japan	Semi-involute	<i>Operculina elegans</i>	7978	7912
<i>Operculina complanata</i>	19543	Sesoko, Japan	Semi-involute	<i>Operculina elegans</i>	9925	8498
<i>Operculina complanata</i>	19544	Sesoko, Japan	Evolute	<i>Operculina elegans</i>	4050	4044
<i>Operculina complanata</i>	19545	Sesoko, Japan	Semi-involute	<i>Operculina elegans</i>	6152	5367
<i>Operculina complanata</i>	19546	Sesoko, Japan	Semi-involute	<i>Operculina elegans</i>	4051	4042
<i>Operculina complanata</i>	19547	Sesoko, Japan	Semi-involute	<i>Operculina elegans</i>	4074	4064
<i>Operculina complanata</i>	19548	Sesoko, Japan	Semi-involute	<i>Operculina elegans</i>	8079	8061
<i>Operculina complanata</i>	19549*	Sesoko, Japan	Semi-involute	<i>Operculina elegans</i>	3562	3546
<i>Operculina complanata</i>	19550	Sesoko, Japan	Evolute	<i>Operculina elegans</i>	3206	3183
<i>Operculina complanata</i>	19551	Sesoko, Japan	Semi-involute	<i>Operculina elegans</i>	7670	6688
<i>Operculina complanata</i>	19552	Sesoko, Japan	Evolute	<i>Operculina elegans</i>	7428	7377
<i>Operculina complanata</i>	19553*	Sesoko, Japan	Evolute	<i>Operculina elegans</i>	12065	11567
<i>Operculina complanata</i>	19555	Sesoko, Japan	Semi-involute	<i>Operculina elegans</i>	8985	8916
<i>Operculina complanata</i>	19556	Sesoko, Japan	Semi-involute	<i>Operculina elegans</i>	7095	7077
<i>Operculina complanata</i>	19557	Sesoko, Japan	Evolute	<i>Operculina elegans</i>	3735	3724
<i>Operculina complanata</i>	19558	Sesoko, Japan	Evolute	<i>Operculina elegans</i>	4530	4523
<i>Operculina complanata</i>	19559	Sesoko, Japan	Evolute	<i>Operculina elegans</i>	6884	6865
<i>Operculina complanata</i>	19560	Sesoko, Japan	Semi-involute	<i>Operculina elegans</i>	8435	8404
<i>Operculina complanata</i>	19561	Sesoko, Japan	Evolute	<i>Operculina elegans</i>	6874	6810
<i>Operculina complanata</i>	19562	Sesoko, Japan	Evolute	<i>Operculina elegans</i>	6563	6531
<i>Neoassilina ammonoides</i>	19506	Sesoko, Japan	Semi-involute	<i>Operculina ammonoides</i>	2589	1836
<i>Neoassilina ammonoides</i>	19524	Sesoko, Japan	Semi-involute	<i>Operculina ammonoides</i>	6614	5328
<i>Neoassilina ammonoides</i>	19525	Sesoko, Japan	Semi-involute	<i>Operculina elegans</i>	3174	3156
<i>Neoassilina ammonoides</i>	19527	Sesoko, Japan	Semi-involute	<i>Operculina ammonoides</i>	4682	3106
<i>Neoassilina ammonoides</i>	19554	Sesoko, Japan	Semi-involute	<i>Operculina elegans</i>	8613	7230
<i>Neoassilina ammonoides</i>	19873	Gulf of Aqaba, Eilat, Israel	Involute	<i>Operculina ammonoides</i>	11235	11210
<i>Neoassilina ammonoides</i>	19897	Gulf of Aqaba, Eilat, Israel	Involute	<i>Operculina ammonoides</i>	6080	5976
<i>Neoassilina ammonoides</i>	19902	Gulf of Aqaba, Eilat, Israel	Semi-involute	<i>Operculina ammonoides</i>	5989	5843
<i>Neoassilina ammonoides</i>	19980	Gulf of Aqaba, Eilat, Israel	Semi-involute	<i>Operculina ammonoides</i>	11173	11087

Table 2 Continued

Species	Isolate	Sampling locality	Test morphology	Morphological identification	Raw reads	Filtered reads
<i>Neoassilina ammonoides</i>	19981	Gulf of Aqaba, Eilat, Israel	Semi-involute	<i>Operculina ammonoides</i>	35541	35305
<i>Neoassilina ammonoides</i>	19985	Gulf of Aqaba, Eilat, Israel	Strong semi-involute	<i>Operculina ammonoides</i>	52692	52131
<i>Neoassilina ammonoides</i>	19986	Gulf of Aqaba, Eilat, Israel	Semi-involute	<i>Operculina ammonoides</i>	44192	43742
<i>Neoassilina ammonoides</i>	19988	Gulf of Aqaba, Eilat, Israel	Involute	<i>Operculina ammonoides</i>	10299	10238
<i>Neoassilina ammonoides</i>	19991	Sesoko, Japan,	Evolute	<i>Operculina ammonoides</i>	3938	3777
<i>Neoassilina ammonoides</i>	19992	Gulf of Aqaba, Eilat, Israel	Semi-involute	<i>Operculina ammonoides</i>	51100	30095
<i>Neoassilina ammonoides</i>	19993*	Gulf of Aqaba, Eilat, Israel	Semi-involute	<i>Operculina ammonoides</i>	88668	88093
<i>Neoassilina ammonoides</i>	20157	Gulf of Aqaba, Eilat, Israel	Evolute	<i>Operculina ammonoides</i>	31370	29352
<i>Neoassilina ammonoides</i>	20158	Gulf of Aqaba, Eilat, Israel	Semi-involute	<i>Operculina ammonoides</i>	3061	3058
<i>Neoassilina ammonoides</i>	20159	Gulf of Aqaba, Eilat, Israel	Semi-involute	<i>Operculina ammonoides</i>	22509	22280
<i>Neoassilina ammonoides</i>	20160	Gulf of Aqaba, Eilat, Israel	Evolute	<i>Operculina ammonoides</i>	6487	6343
<i>Neoassilina ammonoides</i>	20161	Gulf of Aqaba, Eilat, Israel	Strong semi-involute	<i>Operculina ammonoides</i>	2069	2066
<i>Neoassilina ammonoides</i>	20162	Gulf of Aqaba, Eilat, Israel	Semi-involute	<i>Operculina ammonoides</i>	54310	53683
<i>Neoassilina ammonoides</i>	20163	Gulf of Aqaba, Eilat, Israel	Semi-involute	<i>Operculina ammonoides</i>	8428	7674
<i>Neoassilina ammonoides</i>	20164	Gulf of Aqaba, Eilat, Israel	Evolute	<i>Operculina ammonoides</i>	57021	56626
<i>Neoassilina ammonoides</i>	20165	Gulf of Aqaba, Eilat, Israel	Evolute	<i>Operculina ammonoides</i>	14652	14595
<i>Neoassilina ammonoides</i>	20167	Gulf of Aqaba, Eilat, Israel	Semi-involute	<i>Operculina ammonoides</i>	35937	33418
<i>Neoassilina ammonoides</i>	20168	Gulf of Aqaba, Eilat, Israel	Semi-involute	<i>Operculina ammonoides</i>	12021	11943
<i>Neoassilina ammonoides</i>	20169	Gulf of Aqaba, Eilat, Israel	Evolute	<i>Operculina ammonoides</i>	7419	7387
<i>Neoassilina ammonoides</i>	20170	Gulf of Aqaba, Eilat, Israel	Evolute	<i>Operculina ammonoides</i>	6556	6375
<i>Neoassilina ammonoides</i>	20171	Gulf of Aqaba, Eilat, Israel	Evolute	<i>Operculina ammonoides</i>	2442	2377
<i>Neoassilina ammonoides</i>	20172	Gulf of Aqaba, Eilat, Israel	Semi-involute	<i>Operculina ammonoides</i>	15888	15345
<i>Neoassilina ammonoides</i>	20173	Gulf of Aqaba, Eilat, Israel	Semi-involute	<i>Operculina ammonoides</i>	2483	2463
<i>Neoassilina ammonoides</i>	20174	Gulf of Aqaba, Eilat, Israel	Semi-involute	<i>Operculina ammonoides</i>	2524	2285
<i>Neoassilina ammonoides</i>	20175	Gulf of Aqaba, Eilat, Israel	Evolute	<i>Operculina ammonoides</i>	22388	22314
<i>Neoassilina ammonoides</i>	20176	Gulf of Aqaba, Eilat, Israel	Evolute	<i>Operculina ammonoides</i>	5657	5640
<i>Neoassilina ammonoides</i>	20177	Gulf of Aqaba, Eilat, Israel	Semi-involute	<i>Operculina ammonoides</i>	4877	4352
<i>Neoassilina ammonoides</i>	20178	Gulf of Aqaba, Eilat, Israel	Semi-involute	<i>Operculina ammonoides</i>	32662	32496
<i>Neoassilina ammonoides</i>	20179	Gulf of Aqaba, Eilat, Israel	Semi-involute	<i>Operculina ammonoides</i>	7517	7183
<i>Neoassilina ammonoides</i>	20180	Gulf of Aqaba, Eilat, Israel	Semi-involute	<i>Operculina ammonoides</i>	50313	49570
<i>Neoassilina ammonoides</i>	20181	Gulf of Aqaba, Eilat, Israel	Evolute	<i>Operculina ammonoides</i>	16678	16462
<i>Neoassilina ammonoides</i>	20182	Gulf of Aqaba, Eilat, Israel	Semi-involute	<i>Operculina ammonoides</i>	3493	3453

*SSU rDNA barcoding sequences were additionally obtained for these specimens.

The logarithmic marginal spirals show similar increase ($\bar{x}_{ammonoides} = 1.36$ with $s = 0.174$, $\bar{x}_{elegans} = 1.43$ with $s = 0.170$) proven by Student's t-test with $p(H_0) = 0.063$. Deviations from ideal spirals are stronger in *O. elegans* compared to the almost perfect spirals in *O. ammonoides*. These deviations can also be detected in deeper living *O. elegans* from 30 m (Hohenegger and Yordanova, 2000, Plate 2, Figs. 7, 9, 11 therein) and 40 m depth (Yordanova and Hohenegger, 2004, Text-Fig. 2/2 therein).

In the investigated specimens, umbilical plugs are larger in *O. ammonoides* than in *O. elegans*. Small papillae following strictly the septa characterize the surface of inner whorls in *O. ammonoides*, which can be combined leading to elevated beams in later whorls. Large, irregularly distributed papillae, following the septa in later whorls characterize the test surface of *O. elegans*. These structures disappear in all whorls of larger tests.

Differences in the embracing of whorls between involute,

semi-involute and evolute were tested with methods described above. Ratios between marginal and umbilical spirals were calculated in dependence of the revolution angles π and fitted by exponential functions. The function characters 'initial ratio' ($\pi = 0$) and 'slope' were studied for differences between *O. ammonoides* and *O. elegans* (Fig. 2). The scatter diagram shows overlapping in both parameters, where the wider distribution of *O. ammonoides* is caused by small to large-sized individuals from different depths, while *O. elegans* is represented only by small-sized individuals from the shallowest sample (23 m at the reef slope) in Sesoko, Japan. Furthermore, percentages of the umbonal radius to the marginal radius at $\pi/2$ and 2π were calculated. The scatter diagram of both variables shows the strong overlapping of both species (Fig. 3). Discriminant analysis based on the characters 'marginal spiral increase', 'initial ratio', 'slope', 'percentages at $\pi/2$ and 2π ' does not allow the differentiation between both species using the embracing of

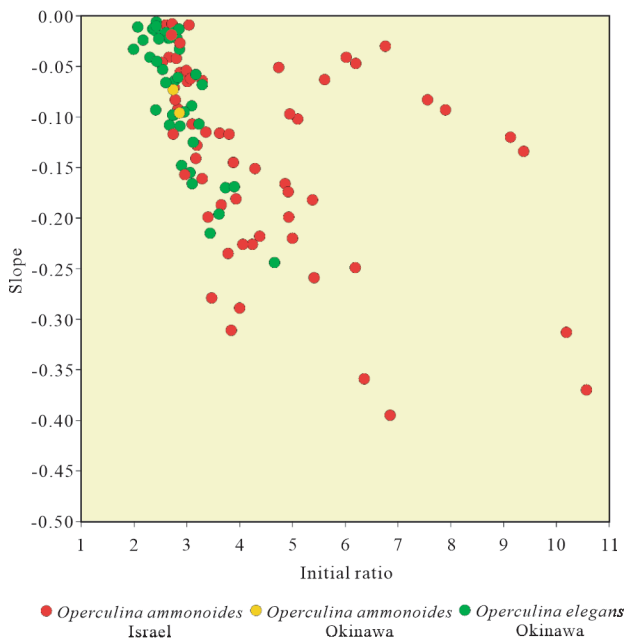


Figure 2. Scatter diagram of the characters 'initial ratio' and 'slope' in Eq. 2.

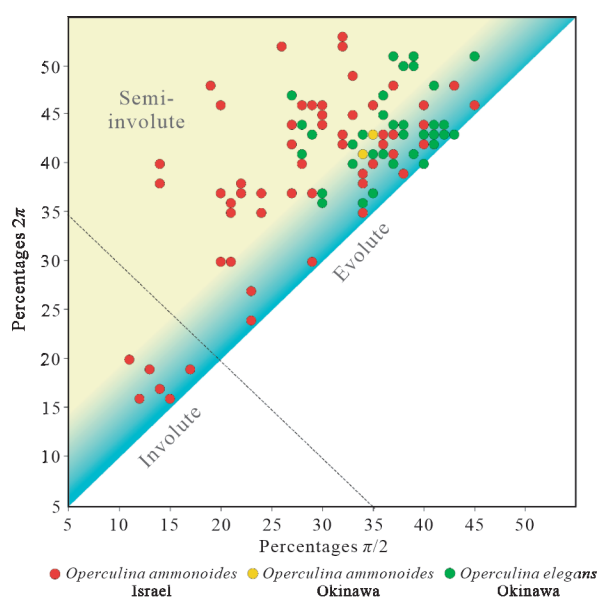


Figure 3. Scatter diagram showing percentages of umbonal on marginal radii at revolution angles $\pi/2$ and 2π .

chambers (Fig. 4). The number of misclassifications using the discriminant function supports this. Of 62 specimens identified as *O. ammonoides*, 25 specimens were classified as *O. elegans* by discriminant analysis. The classification of *O. elegans* obtained better results. Only four out of 41 individuals were classified as *O. ammonoides*.

2.2 Taxonomy

Differentiation between *O. ammonoides* and *O. elegans* is impossible based on characters solely describing the grade of embracing, but septal form, backward bending of chambers together with surface structures like the arrangement and size of pillars, knobs, pustules and beams leads, together with molecular criteria, to the following new classification.

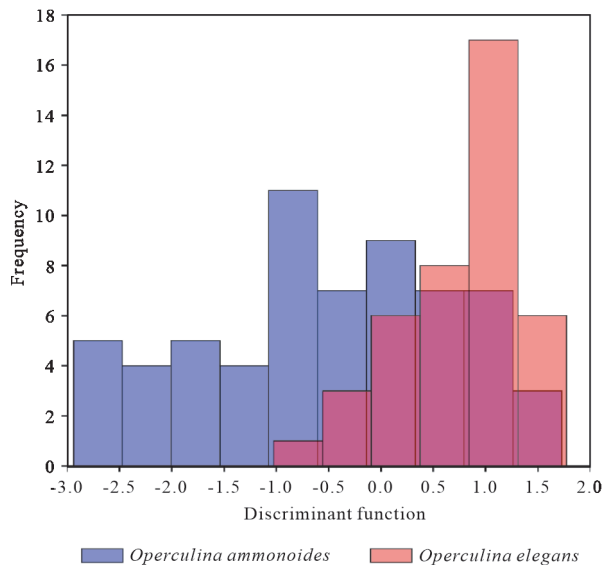


Figure 4. Distribution of *O. ammonoides* (now *Neoassilina ammonoides*) and *O. elegans* along the discriminant function based on the characters 'marginal spiral increase', 'initial ratio', 'slope', '100 (umbonal radius/marginal radius) at $\pi/2$ ' and '100 (umbonal radius/marginal radius) at 2π '.

Supergroup: Rhizaria (Cavalier-Smith 2002)

Phylum: Foraminifera (d'Orbigny 1826)

Class: Globobulimina (Pawlowski et al., 2013)

Family: Nummulitidae (de Blainville, 1827)

Genus: *Operculina* d'Orbigny, 1826

The original description by d'Orbigny is 'Coquille libre, régulière, déprimée; spire régulière, également apparenté de chaque côté; ouverture en fente contre l'avant-dernier tour de spire'. In the revised diagnosis by Loeblich and Tappan (1988), the initial text parts are: 'Test planispiral and evolute, flattened, of medium to large size, numerous narrow chambers in many rapidly expanding whorls, sutures strongly curved back at the periphery. Septal flap moderately to strongly folded laterally'. Hottinger (1977) separated species with strongly folded septa as a different genus named *Planoperculina*.

The type species following the genus diagnosis was originally described from the Oligocene, erroneously stated by Cushman (1914) for recent individuals from the Philippines.

Operculina complanata (Defrance, 1822)

Shallow water specimens are characterized by semi-involute tests, where flat knobs cover the surface of inner windings, becoming large bosses at the umbilicus. These pustules are independent from septal courses, but smaller knobs can be found on septal elevations of lateral test sides. Tests become flat and strongly evolute in deeper-water individuals, where slight septal folding increases with depth. In large specimens, septa are marked on test surface with tiny knobs and chamber walls are covered with pustules.

Molecular features: Complete SSU rDNA sequences contain 3 287 and 3 383 nucleotides (nt), with a GC content of 41.9% and 42.2%, respectively. The length of barcoding sequences ranges from 984 to 994 nt, the GC content ranges from 43.5% to 44.2%. Three different ribotypes have been observed by HTS analysis. Ribotypes are distinguished by 9 sub-

stitutions in the 37F variable region and share the conserved regions at the beginning and the end of this variable zone.

Assilina d'Orbigny, 1839

The original diagnosis by d'Orbigny (1839) 'Tours de spire embrasants seulement dans le jeune age, puis apparents, sans appendices au pourtour' does not help to differentiate *Assilina* from *Operculina*. The genus diagnosis following Loeblich and Tappan (1988) starts with 'Test large, flattened, may be involute but more commonly evolute, with rapidly enlarging whorls and numerous chambers per whorl, sutures radial, slightly curved back at the periphery, imperforate and may be elevated, septa simple, septal flap unfolded.

The type species is the Paleogene *Assilina depressa* d'Orbigny, pictured by Fornasini (1903), and differentiated from the contemporary *Nummulites* by flat, semi-involute to evolute tests. It contradicts the diagnosis of *Assilina* by Loeblich and Tappan (1988) in test shape following a stepwise changing Archimedean spiral where the whorls height keep constant at subsequent growth stages (Hohenegger, 2018) that is typical for Paleogene representatives of both *Assilina* and *Nummulites*. Therefore, the genus diagnosis of *Assilina* by Loeblich and Tappan (1988) is not supported by the type species and its Paleogene representatives (Schaub, 1981). *Operculina ammonoides* (Gronovius) dedicated to *Assilina* by Loeblich and Tappan, could not be assigned to that genus due to the different test construction exercising strong logarithmic spiral growth. Because of these morphological differences, a new genus has to be established.

Neoassilina new genus

Type species: *Nautilus ammonoides* Gronovius 1781

Diagnosis: Planispiral discoidal to flattened tests, semi-involute to evolute, with rapidly enlarging whorls following a logarithmic spiral; sutures radial and slightly curved back at the periphery; septa simple, septal flap unfolded.

Differences: *Neoassilina* is differentiated from *Assilina* by test growth following a logarithmic spiral with rapidly enlarging chambers, while the Paleogene *Assilina* is distinguished by test growth following an Archimedean spiral keeping chamber height constant in subsequent growth stages. *Neoassilina* is differentiated from *Operculina* possessing radial sutures with slight back bending at the periphery, while complete back curving of chambers is characteristic for *Operculina*.

Neoassilina ammonoides (Gronovius, 1781)

Tests are semi-involute in shallow living individuals, becoming strongly evolute in deeper living specimens. This tendency is coupled with test thickness. Starting with thick, discoidal tests, they become flattened in light depleted environments. Expansion rates of the test spiral increase with depth, as does the backbend curving of chambers. Large umbilical plugs surrounded by tiny knobs following the sutures characterize shallow specimens. These knobs can disappear in final whorls of deeper living individuals or can be combined to beams following the suture lines.

Molecular features: Complete SSU rDNA sequences contain 3 381 and 3 388 nt with a GC content of 42.1% and 41.7%, respectively. The length of barcoding sequences ranges

from 983 to 995 nt, the GC content ranges from 43% to 44.1%. Five different ribotypes have been detected by HTS analysis. Ribotypes are distinguished by 11 substitutions in the 37F variable region and share the conserved regions at the beginning and the end of this variable zone.

2.3 High Throughput Sequencing Analysis

In total, 79 specimens were sequenced on high-throughput sequencing technology. The 1'037'727 good quality sequences that were obtained for all specimens grouped into 101 amplicon sequence variants (ASVs). The number of reads per sample is presented in Table 2. After removal of low-reads ASVs (below 100) and contaminants, 61 ASVs were left for the analysis that correspond to the most abundant ASVs (96.6%) of the reads. The retained 61 ASVs were clustered into eight different ribotypes. The relative abundance of each ribotype per specimen is shown in Fig. 5. One group is composed of five ribotypes that are shared within the *Neoassilina ammonoides* specimens. The other group is represented by three different ribotypes that correspond to the species *Operculina complanata*. Ribotypes of *Neoassilina* and *Operculina* are strictly specific and not shared between the two genera.

2.4 Phylogenetic Analysis

The obtained sequences were added to existing databases using the Muscle automatic alignment option as implemented in Seaview vs. 4.3.3. The alignment of partial SSU rDNA sequences corresponding to the barcoding fragment consists of 64 sequences of which 35 were obtained for the present study. It contains 1 046 analyzed sites, nucleotide frequencies are 0.24 (A), 0.21 (C), 0.22 (G), 0.33 (T). The alignment of complete SSU rDNA contains 12 sequences of which 5 were obtained for the present study and consists of 3 649 analyzed sites. Nucleotide frequencies are 0.28 (A), 0.21 (C), 0.20 (G) and 0.31 (T).

Phylogenetic trees were constructed using maximum likelihood phylogeny (PhyML 3.0) as implemented in ATGC: PhyML (Guindon et al., 2010). An automatic model selection by SMS (Lefort et al., 2017) based on Akaike information criterion (AIC) was used, resulting in a GTR + G + I model being selected for both analyses. Initial trees are based on BioNJ. Bootstrap values (BV) are based on 100 replicates.

The phylogenetic tree based on 64 SSU rDNA barcoding sequences is presented in Fig. 6. It contains five clades of nummulitids and is rooted in *Pararotalia nipponica*. *Operculina complanata* (70% BV) and *Palaeonummulites venosus* (91% BV) cluster at the base of other nummulitids, their branching is supported by 82% BV. *Planostegina longisepta*, *Planostegina operculinoides* and *Planoperculina heterosteginoides* build a monophyletic group (82% BV). *Cycloclypeus carpenteri* (100% BV) branches at the base of two clades (80% BV), one containing *Heterostegina depressa* (99% BV), the other consisting of *Operculinella cumingii* (96% BV) and *Neoassilina ammonoides* (75%).

A phylogenetic tree based on 12 complete SSU rDNA sequences is shown in Fig. 7a. The tree is rooted in *P. nipponica* and shows a similar branching of nummulitids. *Palaeonummulites venosus* and *O. complanata* branch again at the base of

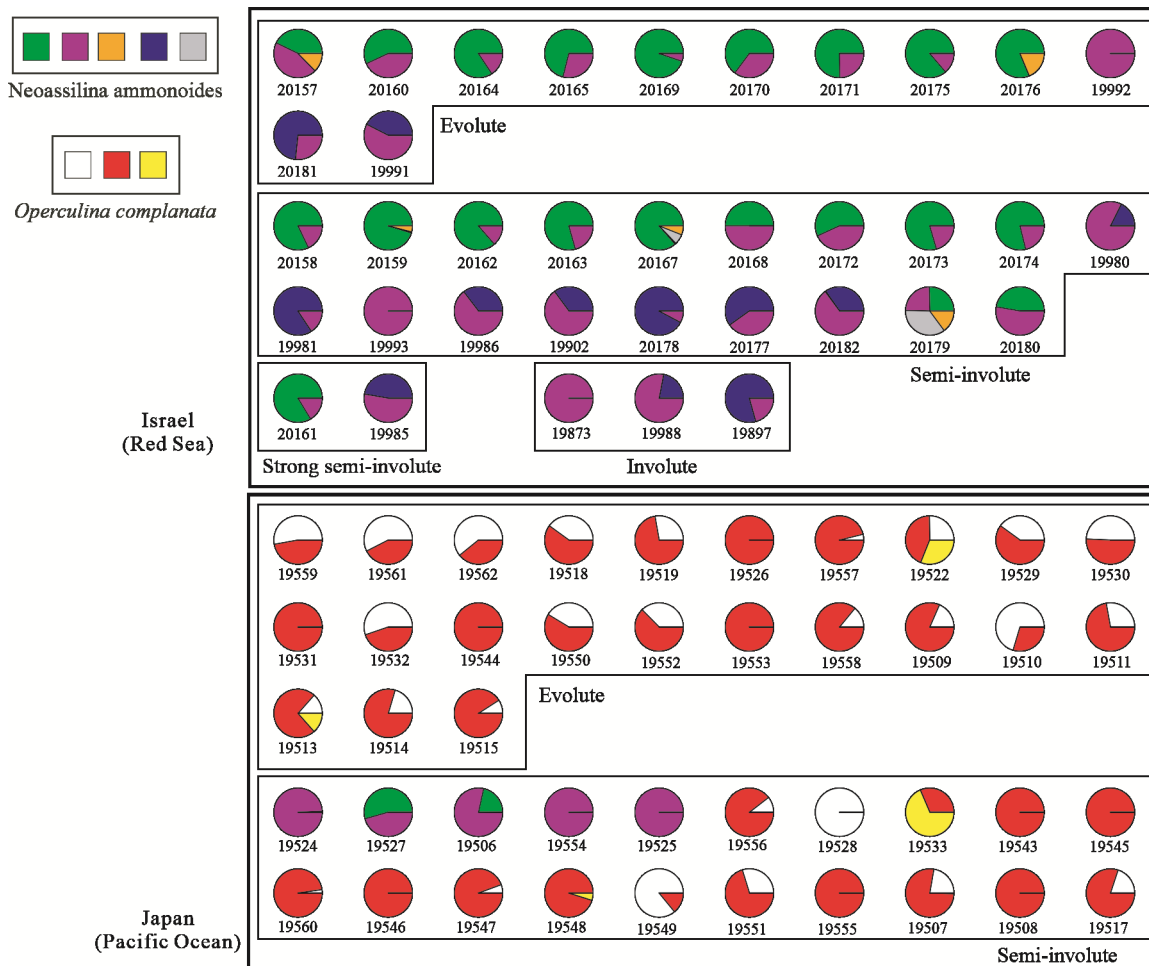


Figure 5. Single cell high throughput sequencing (HTS) analysis of partial SSU rDNA sequences of *Neoassilina ammonoides* (41 specimens) and *Operculina complanata* (38 specimens). Different ribotypes are characterized by their colors. *Neoassilina* and *Operculina* have been separated according to their sampling sites and test morphologies.

other nummulitids (98% BV) followed by the monophyletic group of *Planoperculina* and *Planostegina* (100% BV). Differences concern the branching of *C. carpenteri* and *O. cumingii* that cluster together and *H. depressa* that branches at the base of *N. ammonoides* (100% BV). The latter group is supported by 82% BV.

3 DISCUSSION

Our phylogenetic and HTS results show that species previously assigned to *Operculina* cluster in two different groups that are not closely related (Figs. 5, 6, 7a). *Operculina* is characterized by different morphotypes that are regarded by some as adaptations to different ecological conditions. Planispiral thick involute and flat evolute tests are adapted to high light and low light environments respectively (Oron et al., 2018; Pecheux, 1995). Hohenegger (2000) and Yordanova and Hohenegger (2004) identified different morphotypes as distinct species based on morphological characters such as septal folding, the thinning of tests and different spiral expansion rates. However, Hohenegger (2011) concluded that the similar test morphology of *O. ammonoides* and *O. discoidalis* and overlapping morphological characteristics of *O. complanata* and *O. elegans* would be an argument for ecophenotypes.

In our study we originally recognized four *Operculina* species based on morphological characters that included *O. ammonoides*, *O. discoidalis*, *O. complanata* and *O. elegans* (Tables 1, 2). The results of our molecular studies show that *O. complanata* and *O. elegans* are genetically identical and the latter therefore becomes a junior synonym of *O. complanata*. *Operculina ammonoides* and *O. discoidalis* also proved to be genetically indistinguishable, which makes *O. discoidalis* a junior synonym of the former. *Operculina ammonoides* is genetically well separated from *O. complanata* and the species is transferred to the new genus *Neoassilina*. Both taxa are characterized by variable test morphologies that include evolute, semi-involute and involute test shapes. *Neoassilina* and *Operculina* are distinguished by septal folding in the latter (Hohenegger, 2011). *Neoassilina ammonoides* displays radial sutures with slight back bending at the periphery, while *Operculina complanata* is characterized by complete back curving of chambers. This morphological criterion is discriminant for the separation of the species.

The HTS analysis revealed the occurrence of five different ribotypes in *Neoassilina ammonoides* and three ribotypes in *Operculina complanata* (Fig. 5). The majority of *N. ammonoides* (36 specimens) was sampled from the Gulf of Aqaba, Eilat

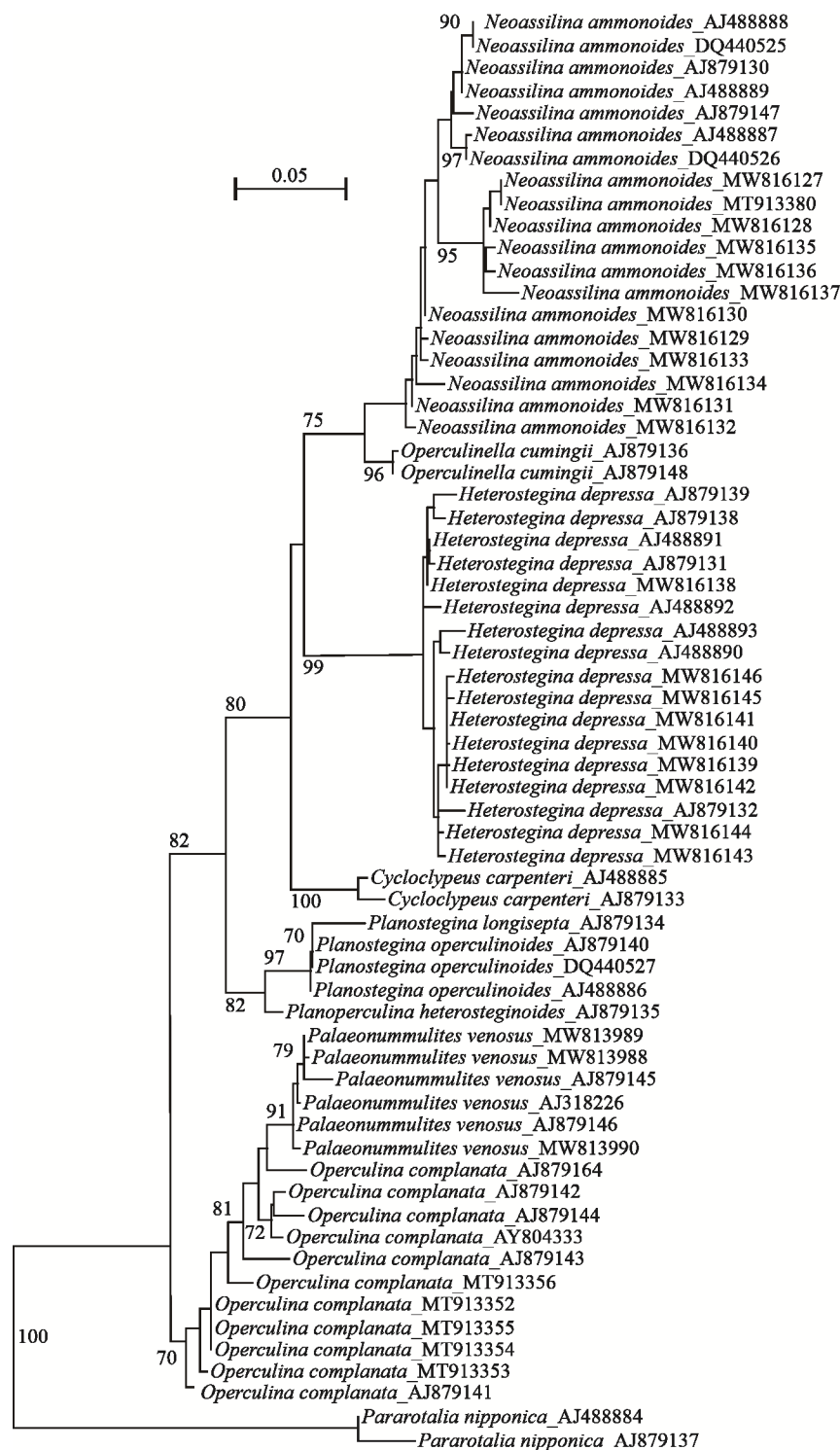


Figure 6. PhyML phylogenetic tree based on the 3' end fragment of the SSU rRNA gene, showing evolutionary relationships of 62 nummulitid taxa. The tree is rooted in *Pararotalia nipponica*. Sequenced specimens are identified by their accession numbers. Numbers at nodes indicate bootstrap values (BV). Only BV larger than 70% are shown.

and five specimens were collected in the Pacific Ocean (Japan, Sesoko). Ribotypes are shared between the Red Sea and Pacific population but the variety is greater in Red Sea specimens with five ribotypes versus two in Pacific *N. ammonoides*. Most individuals (32) have two ribotypes of which one is dominant. In six individuals only one ribotype was found and a minority had either three or four ribotypes (two and one specimen re-

spectively). The investigated *Operculina complanata* (38 specimens) were all sampled from Japan (Sesoko), the species is absent in the Red Sea and the Indian Ocean (Hohenegger, 2006). Most *Operculina* specimens (26) are characterized by two ribotypes, one being more frequent than the other and only few individuals (2) have three ribotypes. Ten *Operculina complanata* possessed one ribotype.

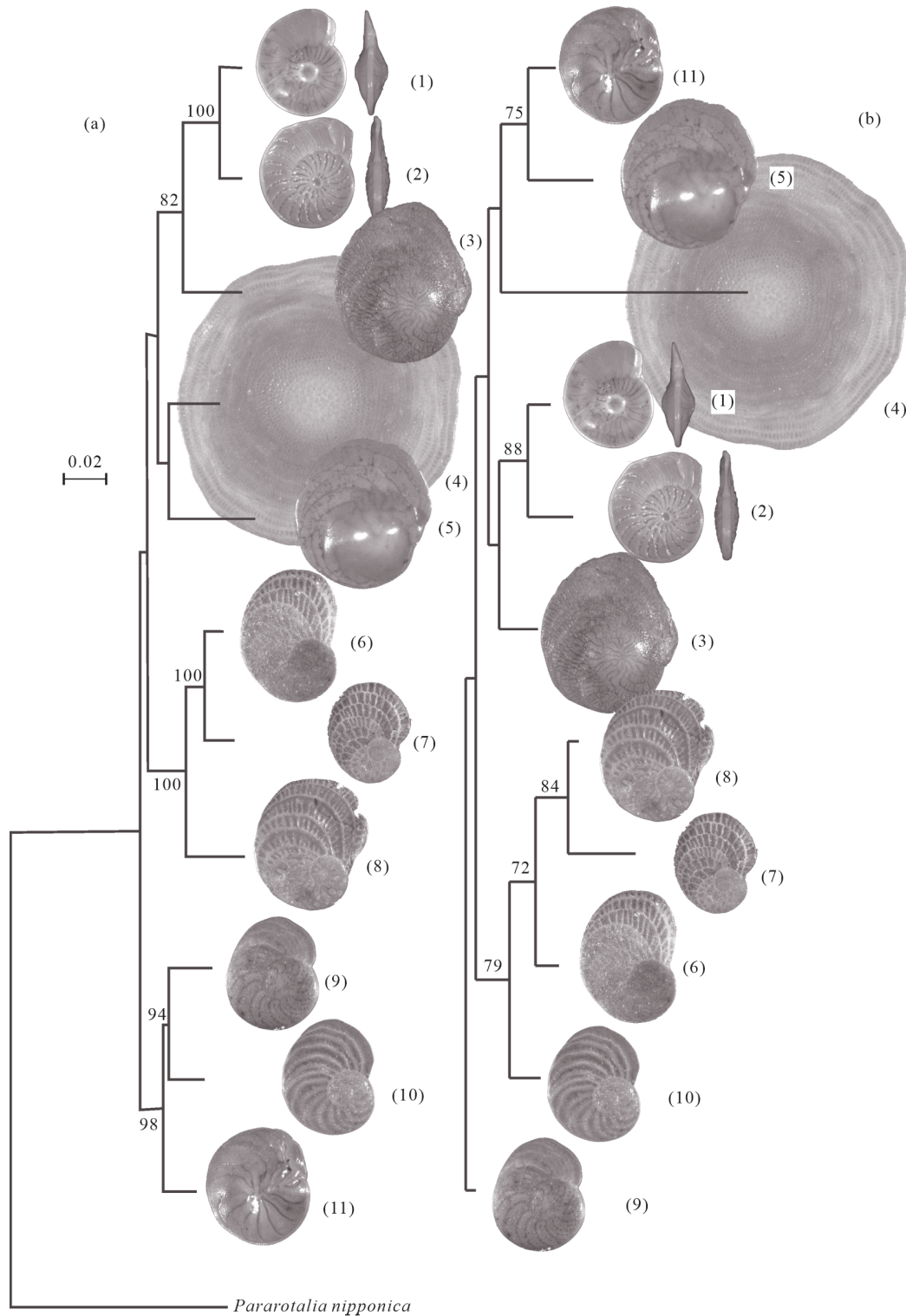


Figure 7. Comparison of molecular and morphological data in Nummulitidae. (a) PhyML phylogenetic tree based on the complete SSU rRNA gene, showing evolutionary relationships of 11 nummulitid taxa. The tree is rooted in *Pararotalia nipponica* (AJ879137). Numbers at nodes indicate bootstrap values (BV). Only BV larger than 70% are shown. (b) Phylogenetic tree based on growth-independent and growth-invariant meristic characters described in Hohenegger (2011, and Table 2 therein) using neighbor joining. Only BV larger than 70% are shown. The tree is rooted in *Operculina complanata*, first described from the Oligocene. All other species are younger, because Paleogene species assigned to *Heterostegina* and *Palaeonummulites* are different from recent forms appearing in the Early Neogene. Numbers correspond to the following species: 1. *Neoassilina ammonoides*, ecophenotype *discoidalis* (AJ879130); 2. *Neoassilina ammonoides*, ecophenotype *ammonoides* (DQ440526); 3. *Heterostegina depressa* (AJ879132); 4. *Cycloclypeus carpenteri* (AJ879133); 5. *Operculinella cumingii* (AJ879136); 6. *Planostegina longisepta* (AJ879134); 7. *Planostegina operculinoides* (DQ440527); 8. *Planoperculina heterosteginoides* (AJ879135); 9. *Operculina complanata*, ecophenotype *elegans* (AJ879164); 10. *Operculina complanata*, ecophenotype *complanata* (AY804333); 11. *Palaeonummulites venosus* (AJ318226). Numbers in brackets refer to sequence accession numbers.

At present, we do not know whether ribotype variability is coupled to phenotypic plasticity or whether it presents an advantage for establishing endosymbiotic relationships with different suitable diatoms, which in turn might provide ecological benefits and more research is needed to investigate these questions.

The phylogenetic relationships of Nummulitidae have been investigated in an earlier study based on five species and partial SSU rDNA and LSU rDNA data (Holzmann et al., 2003). Our current study includes nine species and complete SSU rDNA sequences for representatives of each species as well as HTS data for two genera, *Operculina* and *Neoassilina*. Nummulitidae with chamber subdivision (*Heterostegina*, *Cycloclypeus*, *Planostegina*, *Planoperculina*) and those with undivided chambers (*Neoassilina*, *Operculinella*, *Operculina*, *Palaeonummulites*) branch in several groups (Figs. 6, 7), confirming the independent evolution of secondary septa in different lineages (Holzmann et al., 2003).

Our phylogenetic analyses reveal that *P. venosus* branches close to *O. complanata*, the clade is at the base of other nummulitids (Figs. 6, 7a). *Palaeonummulites* has been referred to *Nummulites* in former publications by some of us (e.g., Hohenegger, 2004, 2000; Holzmann et al., 2003). Torres-Silva et al. (2019) distinguish recent *Palaeonummulites* from extinct *Nummulites* by their enrolment, which follows a logarithmic spiral in extant and Paleogene representatives of *Palaeonummulites*, while the enrolment of *Nummulites* follows an Archimedean spiral. Based on these morphological differences, we comply with their nomenclature.

Analysis of partial SSU rDNA sequences (Fig. 6) that range from 983 to 1 014 nt shows that *P. venosus* and *O. complanata* are paraphyletic. The group is supported by weak bootstrap support (70%) and the paraphyletic clustering might be due to lack of resolution. Analysis of entire SSU rDNA sequences (Fig. 7a) that range from 3 166 to 3 460 nt shows that *P. venosus* and *O. complanata* are a strongly supported sister group (98% BV). The genetic evidence therefore depicts a close relation between *Palaeonummulites* and *Operculina*. However, the monophyly of *P. venosus* and *O. complanata* is not supported by morphology as neither ornamentation, with *P. venosus* distinguished by smooth tests and *O. complanata* showing small but rare papillae, nor test thickness and the grade of backbend angles in chamber form are comparable (Hohenegger, 2011). There is also a pronounced morphological difference in the embrace of whorls. While the thick *P. venosus* tests are completely involute, the flat to extremely flat *O. complanata* starts from semi-evolute tests in shallower regions to completely evolute tests in regions with low light. Additionally, septal folding, characteristic for deeper living *O. complanata*, is absent in *P. venosus* that displays straight, unfolded septa.

The fossil genus *Neonummulites* (Mukhopadhyay, 2016) displays evolute chambers and evolute whorls in juvenile stages and involute chambers and whorls with trabeculae, septal filaments and moderately thick marginal cord in mature stages. Juvenile tests possess some distinctive characters of *Operculina* like nummulitines, while mature tests resemble involute *Nummulites*. Mukhopadhyay (2016) suggests that *Neonummulites* possibly represents a phylogenetic link between the two

genera. Similarly, the ancestor of *Palaeonummulites venosus* and *Operculina complanata* could have displayed characters of both genera with morphological separation taking place during evolution.

A phylogenetic tree based on growth-independent and growth-invariant morphological characters (Hohenegger, 2011, Table 2 therein) shows that *Palaeonummulites venosus* branches as sister to *Operculinella cumingii* (75% BV) with *C. carpenteri* at their base (Fig. 7b). *Operculinella cumingii* branches either as sister to *N. ammonoides* (75% BV) in our molecular analyses (Fig. 6) or as sister to *C. carpenteri* (Fig. 7a). Further studies are necessary to clarify the relationships of *Palaeonummulites*, *Operculina* and *Operculinella* and whether convergent evolution of morphological features in *Palaeonummulites* and *Operculinella* plays a role. *Planostegina* and *Planoperculina* build a monophyletic group supported by strong BV (82%, 100%) in both molecular analyses and are also sustained as a monophyletic group (79%) in the morphological analysis (Fig. 7b). *Planostegina longisepta* differs from *Planostegina operculinoides* by its test surface: chamberlet walls are marked by flat ellipsoidal elevations only in the peripheral chambers while distinct elevations of septa and septula are prominent features in *P. operculinoides*. Surface ornamentations such as knobs or pustules are rare or absent in *P. longisepta* but abundant in *P. operculinoides*. *Planoperculina* is distinguished from *Planostegina* by an incomplete division of chambers into chamberlets and exhibits different sized knobs on its surface (Yordanova and Hohenegger, 2004; Hohenegger and Yordanova, 2000). According to Banner and Hodgkinson (1991), *Planostegina* evolved from *Planoperculina*-like *Operculina* species, that gradually developed secondary septa. Our molecular results confirm the close relationship of the two genera.

Heterostegina and *Cycloclypeus* are also characterized by the possession of secondary chamberlets. In our molecular analyses, *H. depressa* branches either as sister to *N. ammonoides* (82% BV, Fig. 7a), a branching that is also supported by the morphological analysis (Fig. 7b), or at the base of *O. cumingii* and *N. ammonoides*, the branching of the latter being weakly supported (75% BV, Fig. 6). Our molecular analyses show that *Cycloclypeus* is either branching separately at the base of *Heterostegina*, *Operculinella* and *Neoassilina* (Fig. 6) or clustering with *Operculinella* (Fig. 7a), but in both cases the branching is not supported. *Cycloclypeus* branches at the base of *Operculinella* and *Palaeonummulites* in the morphological analysis, but the branching is not supported by BV (Fig. 7b). Early representatives of *Heterostegina* and *Neoassilina* are morphologically very similar and secondary septa developed gradually as shown by intermediate forms (Papp and Küpper, 1954). *Neoassilina*, *Heterostegina* and *Cycloclypeus* share the possession of vertical sutural canals that are forked in *Neoassilina* and undivided in the latter two genera (Hottinger, 1977). Morphological similarities between *O. cumingii* and *H. depressa* can be found in test thickness and its deceleration rate together with the grade of chambers backbend (Hohenegger, 2011). Test thickness and deceleration rate are also similar with *C. carpenteri* and *N. ammonoides* and quite different from *O. complanata*.

4 CONCLUSIONS

We recognize eight different genera in recent Nummulitidae based on molecular and morphological investigations. *Neoassilina* and *Operculina* are two well distinguished genera characterized by variable test shapes adapted to different ecological conditions. They contain a number of different ribotypes that are shared between individuals of the same species and, in the case of *Neoassilina*, also between Red Sea and West-Pacific populations. *Palaeonummulites* and *Operculina* branch together at the base of other nummulitids. *Planostegina* and *Planoperculina* build a monophyletic clade with strong support. *Heterostegina* is related to *Neoassilina*. The position of *Cycloclypeus* and *Operculinella* in phylogenetic trees is variable and more data are needed to establish their exact relationship with other nummulitids.

Our study shows that a combination of molecular and morphological data is necessary to answer the question of ecophenotypes versus species in Nummulitidae.

The genetic homogeneity within nummulitid genera is coupled with a high phenotypic plasticity that allows members of this group to adapt to different environmental conditions. Morphological variability has also been observed in fossil lineages and is attributed to paleoenvironmental changes. The potential for phenotypic plasticity might therefore have implications for the future success of Nummulitidae in view of ongoing climate change.

ACKNOWLEDGMENTS

The current study was supported by Israel Science Foundation (No. 1267/21) to Sigal Abramovich and the Swiss National Science Foundation (No. 31003A_179125) to Jan Pawłowski. Open Access funding provided by University of Geneva. The final publication is available at Springer via <https://doi.org/10.1007/s12583-021-1595-8>.

Open Access This article is licensed under a Creative Commons Attribution 4.0 International License, which permits use, sharing, adaptation, distribution and reproduction in any medium or format, as long as you give appropriate credit to the original author(s) and the source, provide a link to the Creative Commons licence, and indicate if changes were made. The images or other third party material in this article are included in the article's Creative Commons licence, unless indicated otherwise in a credit line to the material. If material is not included in the article's Creative Commons licence and your intended use is not permitted by statutory regulation or exceeds the permitted use, you will need to obtain permission directly from the copyright holder. To view a copy of this licence, visit <http://creativecommons.org/licenses/by/4.0/>.

REFERENCES CITED

- Banner, F. T., Hodgkinson, R. L., 1991. A Revision of the Foraminiferal Subfamily Heterostegininae. *Revista Espanola de Micropaleontologica*, 13(2): 101–140
- Beavington-Penney, S. J., Racey, A., 2004. Ecology of Extant Nummulitids and other Larger Benthic Foraminifera: Applications in Palaeoenvironmental Analysis. *Earth-Science Reviews*, 67(3/4): 219–265. <https://doi.org/10.1016/j.earscirev.2004.02.005>
- Callahan, B. J., McMurdie, P. J., Rosen, M. J., et al., 2016. DADA2: High-Resolution Sample Inference from Illumina Amplicon Data. *Nature Methods*, 13(7): 581–583. <https://doi.org/10.1038/nmeth.3869>
- Cavalier-Smith, T., 2002. The Phagotrophic Origin of Eukaryotes and Phylogenetic Classification of Protozoa. *International Journal of Systematic and Evolutionary Microbiology*, 52(2): 297–354. <https://doi.org/10.1099/00207713-52-2-297>
- Cushman, J. A., 1914. A Monograph of the Foraminifera of the North Pacific Ocean Pt. 4: Chilostomellidae, Globigerinidae, Nummulitidae. *Bulletin of the United States National Museum*, 71(4): 1–46. <https://doi.org/10.5479/si.03629236.71.4>
- d'Orbigny, A., 1839. Foraminifères, in de la Sagra R., Histoire Physique, Politique et Naturelle de l'île de Cuba. A. Bertrand, Paris. 1–224
- d'Orbigny, A., 1826. Tableau Méthodique de la Classe des Céphalopodes. 3ème ordre-Foraminifères. Annales du Muséum d'Histoire Naturelles, Paris. 7: 1–275
- de Blainville, H. M. D., Prêtre, J. G., Turpin, P. J. F., 1827. Manuel de Malacologie et de Conchyliologie. F. G. Levrault, Paris. 1–644. <https://doi.org/10.5962/bhl.title.11582>
- Defrance, J. L. M., 1822. Dictionnaire des Sciences Naturelles. F. G. Levrault, Paris, Strassbourg. 25: 453
- Dufresne, Y., Lejzerowicz, F., Perret-Gentil, L. A., et al., 2019. SLIM: A Flexible Web Application for the Reproducible Processing of Environmental DNA Metabarcoding Data. *BMC Bioinformatics*, 20(1): 88. <https://doi.org/10.1186/s12859-019-2663-2>
- Esling, P., Lejzerowicz, F., Pawłowski, J., 2015. Accurate Multiplexing and Filtering for High-Throughput Amplicon-Sequencing. *Nucleic Acids Research*, 43(5): 2513–2524. <https://doi.org/10.1093/nar/gkv107>
- Fornasini, C., 1903. Illustrazione di Specie Orbignyane di «Nummulitidae» Istituite nel 1826. *Bollettino della Società Geologica Italiana*, 22: 395–397
- Gouy, M., Guindon, S., Gascuel, O., 2010. SeaView Version 4: A Multiplatform Graphical User Interface for Sequence Alignment and Phylogenetic Tree Building. *Molecular Biology and Evolution*, 27(2): 221–224. <https://doi.org/10.1093/molbev/msp259>
- Gronovius, L. T., 1781. Zoophylacii Gronoviani. *Haak et Cie*, 3: 241–380
- Guindon, S., Dufayard, J. F., Lefort, V., et al., 2010. New Algorithms and Methods to Estimate Maximum-Likelihood Phylogenies: Assessing the Performance of PhyML 3.0. *Systematic Biology*, 59(3): 307–321. <https://doi.org/10.1093/sysbio/syq010>
- Hammer, Ø., 2021. PAST. Paleontological Statistics, Version 4.06. [2021-8-6]. http://priode.bf.lu.lv/ftp/pub/TIS/datu_analize/PAST/4.xx/past-4.06-manual.pdf
- Hohenegger, J., 2000. Coenoclines of Larger Foraminifera. *Micropaleontology*, 46(Suppl. 1): 127–151
- Hohenegger, J., 2004. Depth Coenoclines and Environmental Considerations of Western Pacific Larger Foraminifera. *Journal of Foraminiferal Research*, 34(1): 9–33. <https://doi.org/10.2113/0340009>
- Hohenegger, J., 2006. Morphocoenoclines, Character Combination, and Environmental Gradients: A Case Study Using Symbiont-Bearing Benthic Foraminifera. *Paleobiology*, 32(1): 70–99. [https://doi.org/10.1666/0094-8373\(2006\)032\[0070:mccaeg\]2.0.co;2](https://doi.org/10.1666/0094-8373(2006)032[0070:mccaeg]2.0.co;2)
- Hohenegger, J., 2011. Growth-Invariant Meristic Characters Tools to Reveal Phylogenetic Relationships in Nummulitidae (Foraminifera). *Turkish Journal of Earth Sciences*, 20: 655–681
- Hohenegger, J., 2018. Foraminiferal Growth and Test Development. *Earth-Science Reviews*, 185: 140–162. <https://doi.org/10.1016/j.earscirev.2018.06.001>

- Hohenegger, J., Yordanova, H. A., 2000. Remarks on West Pacific Nummulitidae (Foraminifera). *Journal of Foraminiferal Research*, 30(1): 3–28. <https://doi.org/10.2113/0300003>
- Holzmann, M., Pawlowski, J., 2017. An Updated Classification of Rotaliid Foraminifera Based on Ribosomal DNA Phylogeny. *Marine Micropaleontology*, 132: 18–34. <https://doi.org/10.1016/j.marmicro.2017.04.002>
- Holzmann, M., Berney, C., Hohenegger, J., 2006. Molecular Identification of Diatom Endosymbionts in Nummulitid Foraminifera. *Symbiosis*, 42: 93–101
- Holzmann, M., Hohenegger, J., Pawlowski, J., 2003. Molecular Data Reveal Parallel Evolution in Nummulitid Foraminifera. *Journal of Foraminiferal Research*, 33(4): 277–284. <https://doi.org/10.2113/0330277>
- Hottinger, L., 1977. Foraminifères Operculiniformes. *Mémoires du Muséum National d'Histoire Naturelle, Paris, Série C*, 40: 1–159
- Hottinger, L., 2006a. The Depth-Depending Ornamentation of some Lamellar-Perforate Foraminifera. *Symbiosis*, 42(3): 141–151
- Hottinger, L., 2006b. Illustrated Glossary of Terms Used in Foraminiferal Research. *Carnets de Géologie, Mémoires*, (2): 1–43. <https://doi.org/10.4267/2042/5832>
- Langer, M., Hottinger, L., 2000. Biogeography of Selected “Larger” Foraminifera. *Micropaleontology*, 46(Suppl. 1): 105–126
- Lee, J. J., McEnery, M. E., Kuile, B. T., et al., 1989. Identification and Distribution of Endosymbiotic Diatoms in Larger Foraminifera. *Micropaleontology*, 35(4): 353–366. <https://doi.org/10.2307/1485677>
- Lefort, V., Longueville, J. E., Gascuel, O., 2017. SMS: Smart Model Selection in PhyML. *Molecular Biology and Evolution*, 34(9): 2422–2424. <https://doi.org/10.1093/molbev/msx149>
- Loeblich, A. R. Jr., Tappan, H., 1988. Foraminiferal Genera and Their Classification. Van Nostrand Reinhold, New York
- Mukhopadhyay, S. K., 2016. *Neonummulites* gen. nov., Representing a Phylogenetic Link between Evolute and Involute Nummulitines. *Micropaleontology*, 62(5): 365–383. <https://doi.org/10.47894/mpal.62.5.03>
- Oron, S., Abramovich, S., Almogi-Labin, A., et al., 2018. Depth Related Adaptations in Symbiont Bearing Benthic Foraminifera: New Insights from a Field Experiment on Operculina Ammonoides. *Scientific Reports*, 8: 9560. <https://doi.org/10.1038/s41598-018-27838-8>
- Papp, A., Küpper, K., 1954. The Genus *Heterostegina* in the Upper Tertiary of Europe. *Contributions from the Cushman Foundation for Foraminiferal Research*, 5(3): 108–127
- Pawlowski, J., Holzmann, M., 2014. A Plea for DNA Barcoding of Foraminifera. *Journal of Foraminiferal Research*, 44(1): 62–67. <https://doi.org/10.2113/gsjfr.44.1.62>
- Pawlowski, J., Lejzerowicz, F., Esling, P., 2014. Next-Generation Environmental Diversity Surveys of Foraminifera: Preparing the Future. *Biological Bulletin*, 227(2): 93–106. <https://doi.org/10.1086/bblv227n2p93>
- Pawlowski, J., Holzmann, M., Tyszka, J., 2013. New Supraordinal Classification of Foraminifera: Molecules Meet Morphology. *Marine Micropaleontology*, 100: 1–10. <https://doi.org/10.1016/j.marmicro.2013.04.002>
- Pecheux, M. J. F., 1995. Ecomorphology of a Recent Largeforaminifer, Operculina Ammonoides. *Geobios*, 28(5): 529–566. [https://doi.org/10.1016/s0016-6995\(95\)80209-6](https://doi.org/10.1016/s0016-6995(95)80209-6)
- Reiss, Z., Hottinger, L., 1984. The Gulf of Aqaba. Ecological Micropaleontology. Springer Verlag, Berlin. 354
- Schaub, H., 1981. Nummulites et Assilines de la Tethys Paléogène. Taxonomie, Phylogénèse et Biostratigraphie. Mémoires de la Société Paléontologique Suisse/Abhandlungen der Schweizerischen Paläontologischen Gesellschaft. 104: 1–236; 105: pl. 1–48; 106: pl. 49–97
- Torres-Silva, A. I., Eder, W., Hohenegger, J., et al., 2019. Morphometric Analysis of Eocene Nummulitids in Western and Central Cuba: Taxonomy, Biostratigraphy and Evolutionary Trends. *Journal of Systematic Palaeontology*, 17(7): 557–595. <https://doi.org/10.1080/14772019.2018.1446462>
- Yordanova, E. K., Hohenegger, J., 2004. Morphoclines of Living Operculinid Foraminifera Based on Quantitative Characters. *Micropaleontology*, 50(2): 149–177. [https://doi.org/10.1661/0026-2803\(2004\)050\[0149:molofb\]2.0.co;2](https://doi.org/10.1661/0026-2803(2004)050[0149:molofb]2.0.co;2)